

<https://doi.org/10.1038/s41538-025-00657-8>

# A moderate lard-included diet reduces fat deposition and inflammation in the adipose tissue



Xiangyan Liu<sup>1</sup>, Sha Liu<sup>1</sup>, Jingwen Wang<sup>1</sup>, Liu Xu<sup>1</sup>, Zhaoqing Hou<sup>1</sup>, Yule Deng<sup>1</sup>, Rui Zhang<sup>1</sup>, Qiurong Xu<sup>1</sup>, Sisi Yan<sup>2</sup>, Xiaowen Li<sup>3</sup>, Lixin Wen<sup>1,4</sup>✉ & Ji Wang<sup>1</sup>✉

A diet high in animal fat is often linked to metabolic diseases like obesity. Nonetheless, the potential benefits associated with moderate consumption of animal fats are often underestimated. Here, we sought to compare the effects of moderate consumption of three types of fats/ oils—lard, camellia seed oil, and peanut oil—on body fat deposition. Unlike studies on high-fat diets, moderate lard intake significantly decreased lipid accumulation compared with vegetable oils in mice. Mechanistically, moderate lard intake elevated the level of serum taurocholic acid (TCA), which promoted the expression of genes related to lipolysis and the polarization of M2 macrophages in adipose tissue. In vitro experiments further confirmed the molecular mechanism underlying TCA's ability to attenuate lipid accumulation in adipocytes while promoting macrophage polarization. These results challenge traditional views on animal fats, showing that consuming lard at recommended levels can benefit metabolism by maintaining adipose tissue balance.

Obesity and its associated comorbidities have emerged as a global health crisis, with overweight and obesity ranking as the fifth leading mortality risk factor worldwide<sup>1,2</sup>. Obesity is strongly influenced by lifestyle, particularly excessive or imbalanced fat intake. Although high-fat diets are often linked to obesity, the prior research suggests that high-carbohydrate, low-fat diets may induce even more significant hepatic cholesterol deposition than high-fat, high-calorie diets<sup>3</sup>. Additionally, purified diets in animal models have long been a cornerstone of obesity research. However, evidence reveals significant inconsistencies compared with studies using whole-food diets<sup>4</sup>. These discrepancies suggest that flawed dietary model designs, such as ultra-high-fat short-term protocols, and inappropriate feed choices, including both purified and whole-food diets, may contribute to contradictory research conclusions. Despite long-standing recommendations in dietary guidelines for Chinese residents to replace saturated fatty acids (SFAs) with unsaturated fatty acids (USFAs), obesity rates in China have continued to rise alongside declining consumption of animal fats<sup>5</sup>. Similarly, comparative studies on ethnic diets reveal paradoxical trends: populations consuming traditional pork- and lard-based diets show significantly lower obesity and diabetes prevalence than those on plant-based or vegetarian diets<sup>6,7</sup>. This paradox highlights the imperative for a more comprehensive understanding of the metabolic

impacts of specific dietary fats and necessitates a critical reevaluation of prevailing nutritional guidelines.

In obesity, adipose tissue dysfunction is marked by enlarged adipocytes, ectopic lipid deposition, and persistent low-grade inflammation, driven by macrophage infiltration and pro-inflammatory cytokine secretion<sup>8</sup>. Enlarged adipocytes undergo metabolic shifts, favoring lipid storage over oxidation, while hypoxia and endoplasmic reticulum stress further exacerbate inflammatory responses<sup>9</sup>. Notably, the interplay between dietary lipids and adipose tissue inflammation remains poorly understood. While high-fat diets typically promote metabolic dysfunction, emerging evidence suggests that certain lipid sources may, paradoxically, alleviate inflammation and enhance metabolic health<sup>10,11</sup>.

Our prior study showed that rising dietary oil consumption and alterations in its composition have contributed to the increased obesity rate in China over recent decades. Notably, a mixture of lard, high in saturated fatty acids (SFAs), and soybean oil, rich in polyunsaturated fatty acids (PUFAs), demonstrated significant anti-obesity effects and mitigated non-alcoholic fatty liver disease (NAFLD)<sup>6,12</sup>. Further studies revealed that, in comparison to lard, soybean oil alone exacerbates neuroinflammation under high-fat dietary conditions through gut-brain axis activation<sup>11</sup>. Additionally, we found that olive oil induced more severe hepatic lipid

<sup>1</sup>Hunan Engineering Research Center of Livestock and Poultry Health Care, College of Veterinary Medicine, Hunan Agricultural University, Changsha, China.

<sup>2</sup>Hunan Province Key Laboratory of Typical Environmental Pollution and Health Hazards, School of Public Health, Hengyang Medical School, University of South China, Hengyang, China. <sup>3</sup>Changsha Agriculture and Rural Affairs Bureau, Changsha, China. <sup>4</sup>Changsha Lvye Biotechnology Co. Ltd., Changsha, China.

✉ e-mail: [sfwlx8015@sina.com](mailto:sfwlx8015@sina.com); [wangjics@163.com](mailto:wangjics@163.com)

deposition under high fat conditions than lard and rapeseed oil. These findings demonstrate that dietary oils with distinct fatty acid profiles have significantly different effects on body lipid metabolism. Consequently, we selected three oils with high MUFA content—lard (which is rich in both SFAs and MUFA), camellia seed oil (predominantly MUFA), and peanut oil (abundant in both PUFAs and MUFA)—to evaluate and compare their effects on lipid deposition in adipose tissue. Furthermore, whole-food diets were used in this study. Although purified diets (e.g., AIN-93) offer better nutritional standardization, we adopted food-grade fat sources to better simulate moderate human consumption patterns, where fat is ingested as part of the entire food matrix rather than an isolated purified component. Therefore, whole-food diets were chosen to reduce the deviation of con-

clusions caused by the “disconnect between the experimental model and real-world scenarios.

## Results

### Dietary lard at 25% energy level reduces adipose tissue accumulation, promotes lean body mass gain, and attenuates oxidative damage

In this study, we detected the fatty acid components of lard (Lar), camellia seed oil (Cam) and peanut oil (Pea) (Table 1 and Fig. 1A), which were as follows: Lar contained 39.47% SFAs (primarily palmitic acid, 24.23%, and stearic acid, 14.28%), 40.47% MUFA (mainly oleic acid, 38.04%), and 19.82% PUFAs (mainly linoleic acid, 18.77%); Cam contained 11.34% SFAs (primarily palmitic acid, 8.08%), 81.28% MUFA (mainly oleic acid, 80.61%), and 7.38% PUFAs (mainly linoleic acid, 7.32%); Pea contained 23.04% SFAs (primarily palmitic acid, 10.29%), 47.66% MUFA (mainly oleic acid, 46.71%), and 29.3% PUFAs (mainly linoleic acid, 29.17%). Further analysis of PUFA subtypes revealed that n-6 PUFAs accounted for the majority of total PUFAs in all three oils, Pea had the highest n-6 PUFA content (29.23%). In comparison, n-3 PUFAs were present at extremely low levels across all oils, with Lar showing a slightly higher proportion (0.14%). Correspondingly, the n-3/n-6 PUFA ratio was highest in Lar. In addition, we revealed significant differences in body weight and lean body mass among the groups. Specifically, the body weight of mice in the Lar group was markedly higher compared with those in the Cam group (Fig. 1B) ( $P < 0.05$ ). However, the lean body mass/body weight (%) in the Lar group was significantly greater than in Cam groups (Fig. 1C) ( $P < 0.05$ ). Despite the absence of a statistically significant difference in the percentage of body fat in all groups, a noticeable trend towards a decrease was observed in the Lar

**Table 1 | Fatty acid composition of oils/fats in groups**

	Lar	Cam	Pea
Fatty acid	The percentage of total fatty acids		
SFAs	39.47	11.34	23.04
MUFAs	40.47	81.28	47.66
PUFAs	19.82	7.38	29.30
n-3 PUFAs	0.14	0.03	0.05
n-6 PUFAs	18.88	7.35	29.23
n-3/n-6	0.007	0.004	0.002

Lar Lard, Cam Camellia seed oil, Pea Peanut oil, SFA Saturated Fatty Acids, MUFA Monounsaturated Fatty Acids, PUFA Polyunsaturated Fatty Acids.

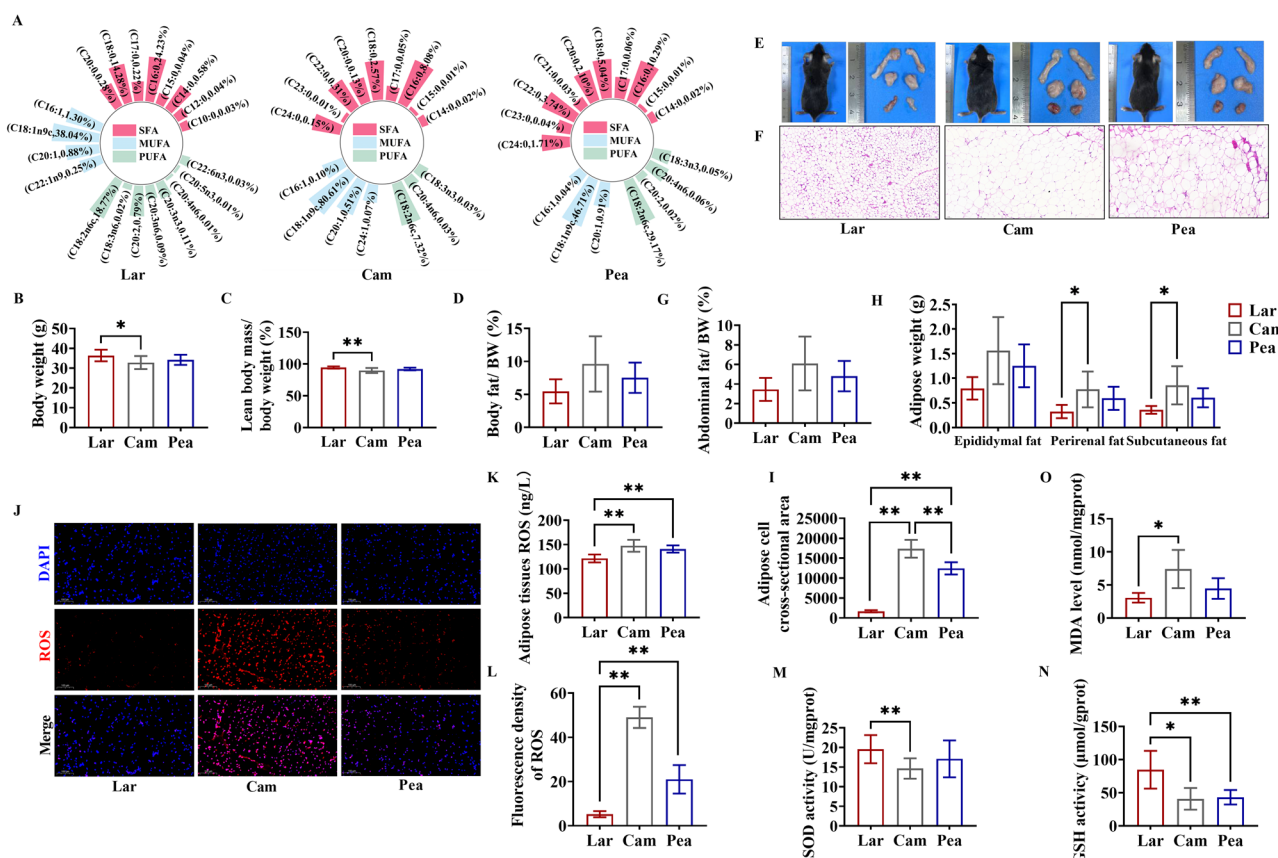


**Fig. 1 | Dietary lard at 25% energy level reduces adipose tissue accumulation and promotes lean body mass.** A Fatty acid composition. B Body weight. C Lean body mass/bw (%). D Body fat/bw (%). E Gross view of the mouse and adipose tissue. F HE staining of subcutaneous fat (200×). G Abdominal fat/BW (%). H Adipose weight. I Adipose cell cross-sectional area. J Immunofluorescence detection of ROS in the subcutaneous fat (100×). K ROS content of the adipose tissue. L Fluorescence intensity statistics of ROS. M SOD activity assay of adipose tissue. N GSH activity assay of adipose tissue. O MDA activity assay of adipose tissue. Lar Lard, Cam Camellia seed oil, Pea Peanut oil.

J Immunofluorescence detection of ROS in the subcutaneous fat (100×). K ROS content of the adipose tissue. L Fluorescence intensity statistics of ROS. M SOD activity assay of adipose tissue. N GSH activity assay of adipose tissue. O MDA activity assay of adipose tissue. Lar Lard, Cam Camellia seed oil, Pea Peanut oil.

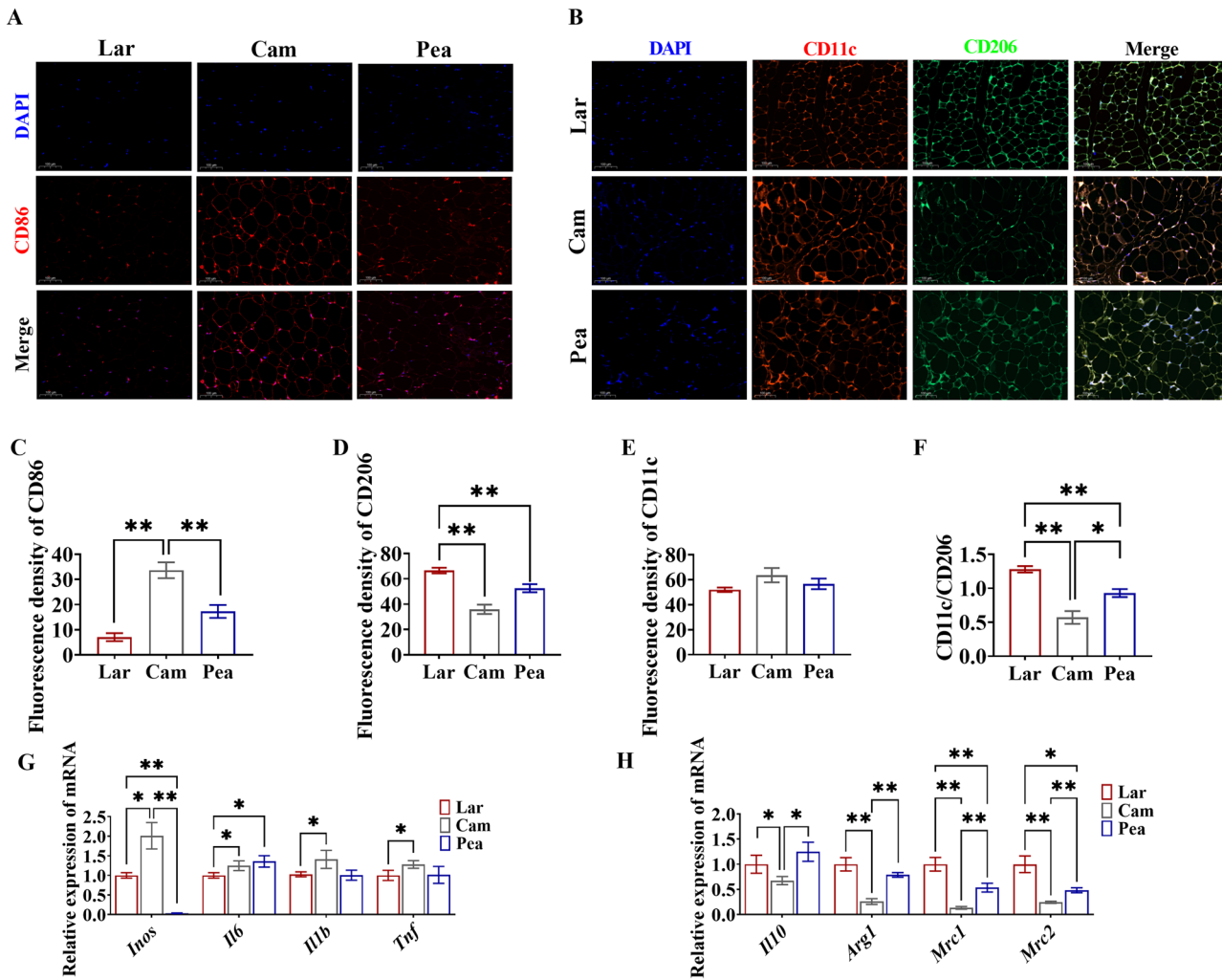


**Fig. 2 | Dietary lard at 25% energy level promotes macrophage M2 polarization and reduces adipose tissue inflammation.** A Immunofluorescence detection of CD86 in the subcutaneous fat (100 $\times$ ). B Immunofluorescence double staining of CD11c and CD206 (100 $\times$ ). C Fluorescence intensity statistics of CD86.

D, E Fluorescence intensity statistics of CD11c and CD206. F CD206/CD11c ratio. G Relative expression of genes characteristic of M1 polarization. H Relative expression of genes characteristic of M2 polarization. Lar Lard, Cam Camellia seed oil, Pea Peanut oil.

group (Fig. 1D). Gross figures and histological examination of adipose tissue show that lard can reduce the size of adipose cells (Fig. 1E-I) ( $P < 0.01$ ). Excessive fat accumulation induced by unbalanced dietary lipids triggers oxidative stress<sup>13</sup>. Immunofluorescence analysis revealed that ROS levels were significantly higher in the Cam and Pea groups compared with the Lar group (Fig. 1J, L), consistent with the data shown in Fig. 1K ( $P < 0.01$ ). Notably, the Lar group exhibited a marked increase in SOD and GSH activities, along with a significant decrease in MDA activity (Fig. 1M-O) ( $P < 0.01$ ,  $P < 0.05$ ), suggesting that lard supplementation enhances antioxidant capacity and mitigates oxidative stress.

#### Dietary lard at 25% energy level promotes macrophage M2 polarization and reduces adipose tissue inflammation

Excessive fat accumulation can further induce adipose inflammation, which is closely associated with macrophages. Our immunofluorescence analysis revealed distinct effects of dietary oils on macrophage polarization (Fig. 2A and B). Compared with the Lar and Pea groups, the expression of M1 macrophage marker CD86 was significantly elevated in the Cam group, but the fluorescence intensity of M2 macrophage marker CD206 was significantly higher in the Lar group than in the Cam and Pea groups (Fig. 2C and D) ( $P < 0.01$ ), although there was no significant difference in CD11c expression, the CD206/CD11c ratio was significantly higher than that in the Cam group (Fig. 2E and F) ( $P < 0.01$ ). M1-related genes (*Inos*, *Il1b* and *Tnf*)

were significantly up-regulated in the Cam and Pea groups, while *Il6* expression was highest in the Pea group and significantly lower in the Lar group (Fig. 2G) ( $P < 0.05$ ). Conversely, the Lar group showed enhanced expression of the anti-inflammatory cytokine *Il10* and M2 polarization markers (*Arg1*, *Mrc1*, *Mrc2*) (Fig. 2H) ( $P < 0.05$ ). These findings collectively indicate that lard preferentially promotes an anti-inflammatory M2 macrophage phenotype, potentially contributing to reduced adipose tissue inflammation.

#### Dietary lard at 25% energy level increases energy metabolism and promotes lipolysis

The Cam group exhibited a significant up-regulation of key lipogenesis genes, such as *Cebpa*, *Fasn*, *Scd1*, and *Dgat2*, all of which were significantly higher than in the Lar and Pea groups. The Pea group showed significantly higher *Srebp1c* expression than the Lar group (Fig. 3A) ( $P < 0.01$ ). In contrast, the expression of lipolysis-related genes *Atgl*, *Hsl*, *Cat*, and *Acs* in the Lar group was significantly higher than that in the Cam and Pea groups. The expression of *Cpt1* was significantly higher than that in the Cam group, suggesting that lard may contribute to the reduction of fat accumulation (Fig. 3B). The results were further confirmed in immunofluorescence (Fig. 3D-F). Regarding non-shivering thermogenic genes in subcutaneous fat, the Cam group showed significantly lower expression of *Ucp1*, *Ampk*, *Ppargc1a*, *Prdm16*, and

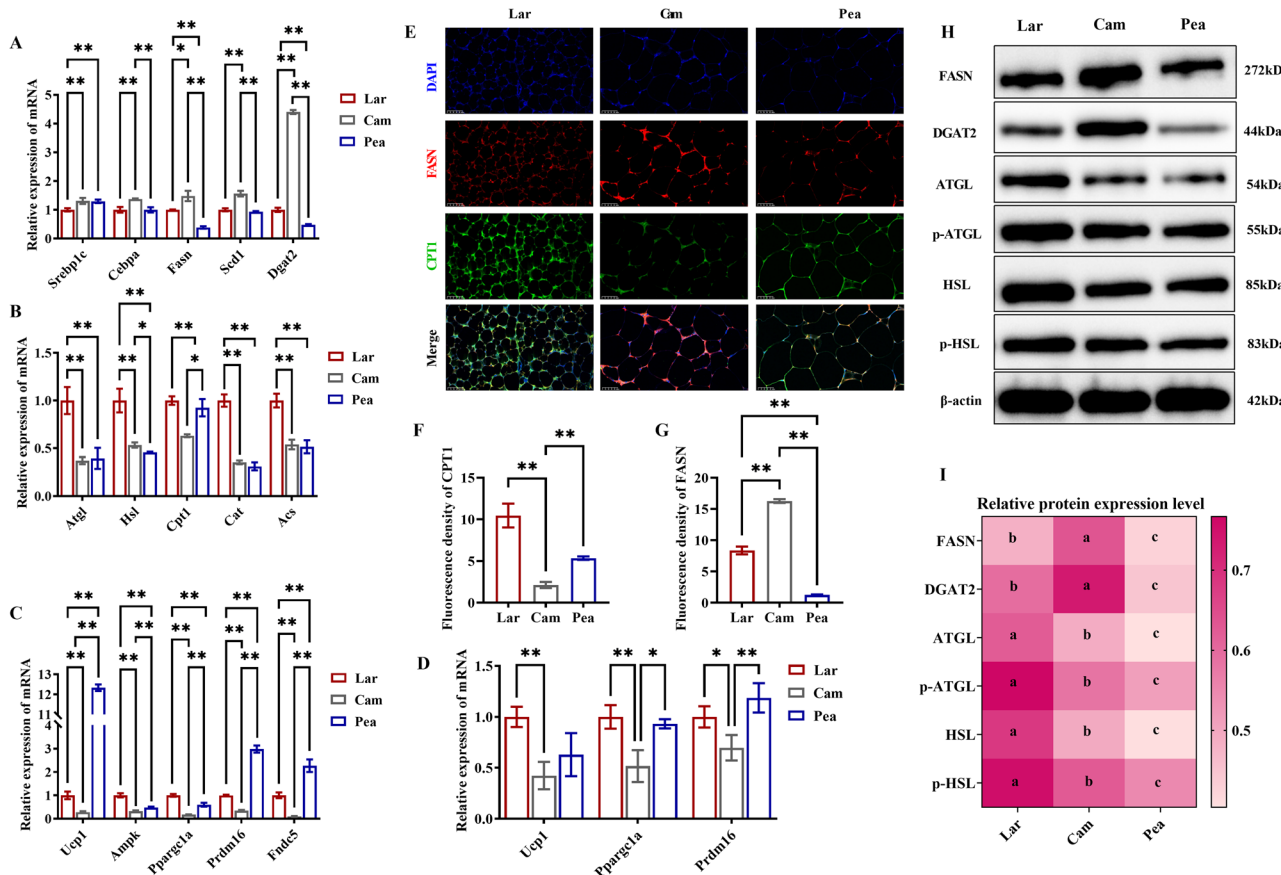


**Fig. 3 | Dietary lard at 25% energy level increases energy metabolism and promotes lipolysis.** A The relative expression of genes for lipogenesis. B The relative expression of genes for lipolysis. C The relative expression of genes related to non-shivering thermogenesis in subcutaneous fat tissue. D The relative expression of genes related to non-shivering thermogenesis in brown adipose tissue.

E Immunofluorescence double staining of FASN and CPT1 (200×).

F, G Fluorescence intensity statistics of FASN and CPT1. H, I Relative protein expressions of FASN, DGAT2, ATGL, P-ATGL, HSL, P-HSL. Lar: Lard, Cam: Camellia seed oil, Pea: Peanut oil. Superscript letters (a, b, c and d) indicate significant differences between groups at  $P < 0.05$ .

*Fndc5* than the Lar and Pea groups. The Pea group showed significantly higher expression of *Ucp1*, *Prdm16* and *Fndc5* than the Lar group, but lower *Ampk* and *Ppargc1a* expression (Fig. 3C) ( $P < 0.01$ ). Furthermore, in brown adipose tissue, the Cam group showed a significantly lower *Ucp1* expression than the Lar group ( $P < 0.01$ ), and a significantly lower *Ppargc1a* and *Prdm16* expression than both the Lar and Pea groups ( $P < 0.05$ ,  $P < 0.01$ ). Western blotting results confirmed that compared with the Cam group, the Lar group downregulated the expression of lipogenesis-related proteins (FASN and DGAT2); compared with the Pea and Cam groups, the Lar group upregulated the expression of lipolysis-related proteins (ATGL, P-ATGL, HSL, and P-HSL) (Fig. 3H-I) ( $P < 0.05$ ). Collectively, these findings indicate that lard controls fat accumulation by promoting lipolysis and non-shivering thermogenesis.

#### Non-targeted metabolomics reveals significant differences in serum metabolites between groups

To investigate the potential mechanisms of different dietary oils on lipid metabolism. Metabolomics analysis was performed, and the results are shown in Fig. 4. We found differences in the composition of metabolites among the three groups (Fig. 4A-F). In view of the positive effect of lard on inhibiting lipid accumulation in the above results, we next performed KEGG pathway enrichment analysis using 85 metabolites with significantly higher abundance in the Lard group vs. the Cam group or the Pea group as the metabolite set (Fig. 4G). Further metabolite classification analysis revealed that lipids and lipid-like molecules accounted for 83.05% of the total metabolites, of which 49 metabolites were particularly

enriched in the lard group (Fig. 4H). A hierarchical cluster analysis of the top 40 metabolites by abundance (Fig. 4I) showed distinct metabolic profiles in the Lard group vs. the Cam and Pea groups, leading to the screening of 12 typical metabolites (Fig. 4J-U). Notably, TCA, a bile acid, is often supplemented into the diet to study its effects on fish and mammals. Exogenous TCA supplementation may modulate bile acid metabolism by enhancing bile acid reabsorption, thereby reducing lipid accumulation<sup>14</sup>. Based on this, we hypothesized that lard in reducing lipid accumulation may be mediated by TCA.

#### TCA promotes lipolysis and M2 macrophage polarization

Next, we further explored the role of TCA in reducing lipid accumulation and alleviating adipose tissue inflammation associated with lard consumption. By correlating differential metabolites with phenotypes related to lipid metabolism and adipose inflammation, we observed that TCA was significantly negatively correlated with adipose cell cross-sectional area (CSA), body fat mass, and subcutaneous fat mass. Conversely, it exhibited a significant positive correlation with lean body mass and genes associated with lipolysis (Fig. 5A). Additionally, levels of reactive ROS, *Il1b*, the CD11c/CD206 ratio, and *Inos* expression were negatively correlated with TCA levels. In contrast, the expression levels of genes related to macrophage M2 polarization and the anti-inflammatory cytokine *Il10* were positively correlated with TCA levels (Fig. 5B). These findings suggest that TCA may play a crucial role in mitigating lipid accumulation and adipose tissue inflammation in lard by modulating lipid metabolism and inflammatory responses.

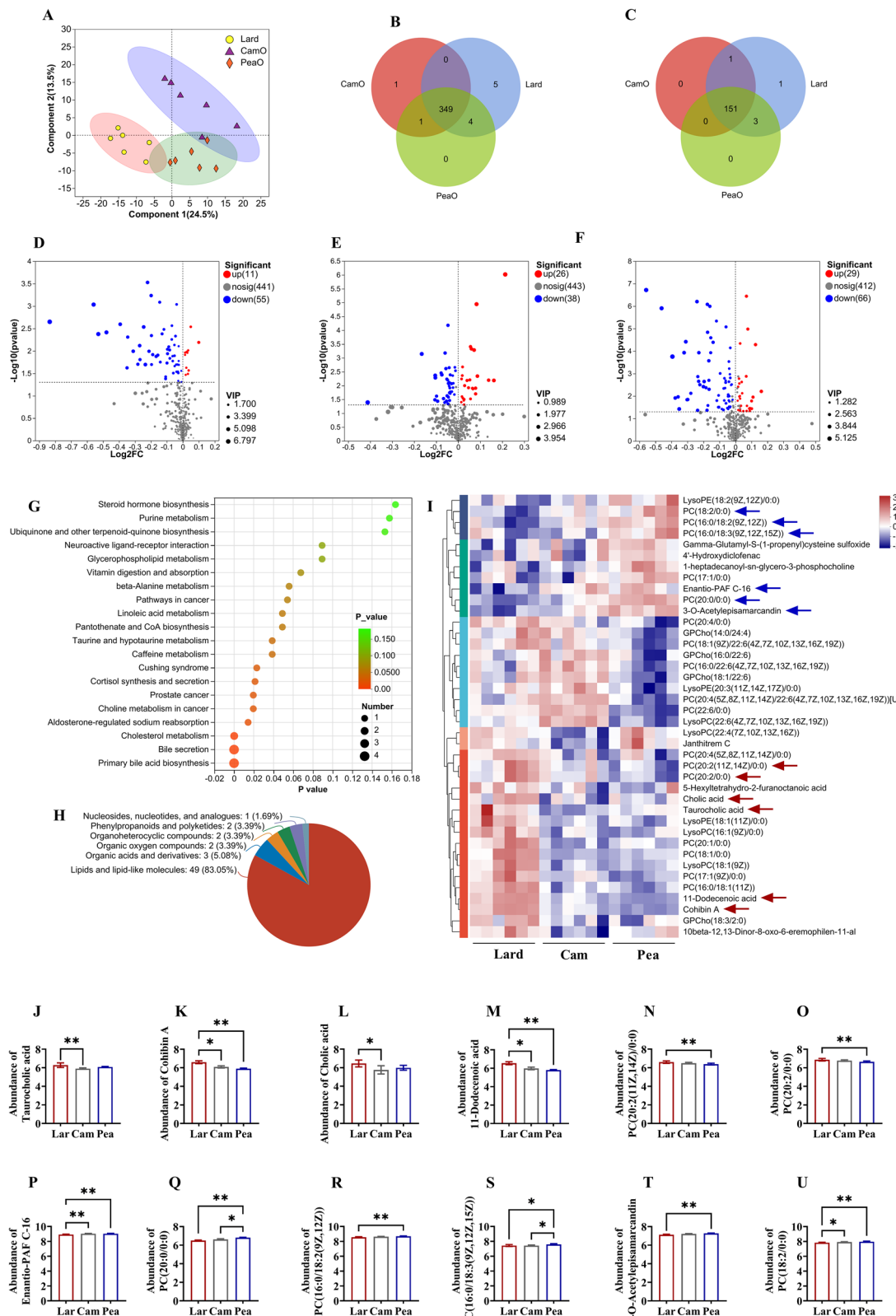


**Fig. 4 | Non-targeted metabolomics reveals significant differences and functional enrichment analysis of serum metabolites between groups. A** Partial least squares-discriminant analysis (PLS-DA). **B** Venn analysis in positive ion mode. **C** Venn analysis in negative ion mode. **D** Volcano plot analysis for CamO vs Lard, **E** PeaO vs Lard, **F** CamO vs PeaO. CamO: Camellia seed oil, PeaO: Peanut oil. **G** KEGG pathway enrichment analysis. **H** Metabolites classified by HMDB database.

**I** Hierarchical clustering analysis of metabolites. Relative metabolite abundances of **J** Taurocholic acid. **K** Cohibin A. **L** Cholic acid. **M** 11-Dodecanoic acid. **N** PC (20:2(11Z,14Z)/0:0). **O** PC (20:2/0:0). **P** Enantio-PAF C-16. **Q** PC (20:0/0:0). **R** PC (16:0/18:2(9Z,12Z)). **S** PC (16:0/18:3(9Z,12Z,15Z)). **(T)** 3-O-Acetylepisamarcandin. **U** PC (18:2/0:0). Lar Lard, Cam Camellia seed oil, Pea Peanut oil.

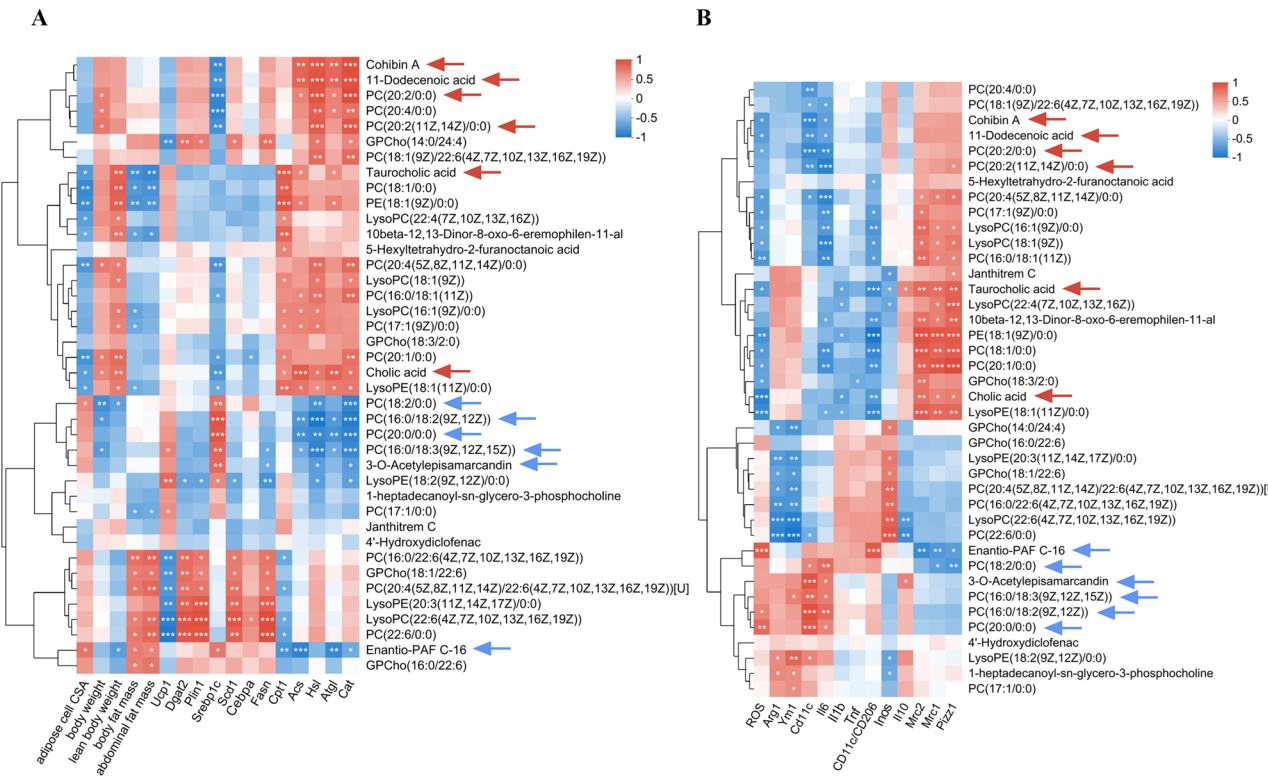


**Fig. 5 | Phenotype-metabolite association analysis. A** Association between adipose tissue metabolism and serum metabolites; **B** Association between adipose tissue inflammation and serum metabolites.

### TCA promotes LPS-induced polarization of RAW264.7 from M1 to M2 type

To explore the impact of TCA on macrophage polarization, we initially assessed the effect of different concentration gradients of TCA on the viability of RAW264.7 cells and found that the highest cellular metabolic activity was observed at 12.5 and 25  $\mu$ M concentrations (Fig. 6A). Using 1  $\mu$ g/ml LPS to induce M1 polarization, we examined TCA's effect (12.5 and 25  $\mu$ M). TCA significantly decreased the levels of IL-1 $\beta$  and NO in RAW264.7 cells after LPS induction (Fig. 6B and C) ( $P < 0.05$ ). Immuno-fluorescence showed TCA reversed LPS-induced CD86 upregulation and enhanced CD206 fluorescence (Fig. 6D-F). Additional analyses revealed that TCA markedly suppressed the expression of pro-inflammatory factors in M1 macrophages, including *Il1b*, *Il6*, *Tnf*, and *Inos* (Fig. 6H-J) ( $P < 0.05$ ), and promoted the expression of markers associated with M2 macrophages, such as *Arg1* and *Il10* (Fig. 6K-L) ( $P < 0.05$ ). Molecular docking showed TCA bound to ARG1 with a high binding affinity (-8.594 kcal/mol) (Fig. 6G). Collectively, these findings suggest that TCA facilitates the transition of M1 macrophages into an anti-inflammatory M2 phenotype.

### TCA inhibits lipogenesis in 3T3-L1 cells

To further investigate the inhibitory effect of TCA on lipid accumulation, 3T3-L1 cells were treated with TCA at 0, 1, 6.25, 12.5, 25, and 50  $\mu$ M. TCA at 12.5 and 25  $\mu$ M significantly enhanced cell metabolic activity (Fig. 7A) ( $P < 0.05$ ). During 3T3-L1 differentiation, TG content decreased in a dose-dependent manner with increasing TCA, and the TCA-25 group showed the most significant reduction (Fig. 7B). Microscopic observation revealed that TCA significantly reduced the accumulation of lipid droplets (Fig. 7C-E) ( $P < 0.05$ ).

For gene and protein expression analysis, immunofluorescence showed TCA reduced FASN fluorescence intensity and increased CPT1 intensity in a dose-dependent manner (Fig. 7F-H) ( $P < 0.05$ ). Western blot and qPCR results confirmed TCA down-regulated lipogenesis-related genes/proteins and up-regulated lipolysis-related genes/proteins (Fig. 7I-K) ( $P < 0.05$ ). Molecular docking analysis revealed that TCA bound to CPT1 via

stable hydrogen bonds and electrostatic interactions (Fig. 7L), with a high binding affinity (-8.148 kcal/mol). Collectively, these findings indicate that TCA modulates lipid metabolism and inhibits lipogenesis in 3T3-L1 cells.

### Dissusion

Research indicates a positive correlation between dietary fat intake and obesity<sup>15</sup>. Our study explored the effects of three MUFA-rich dietary oils, lard, camellia seed oil, and peanut oil, on lipid metabolism. Despite their similar high MUFA content, the animal fat (lard) and vegetable oils (camellia seed oil and peanut oil) exhibited significant differences in regulating body weight and fat mass, which may be attributed to specific variations in fatty acid composition (e.g., SFA proportion, n-3/n-6 PUFA ratio, and PUFA subtype content) and bioactive components. Lard, a traditional animal fat in China, was found in our previous research to reduce obesity incidence when combined with soybean oil<sup>6</sup>. Although lard contains high MUFA (40.47%, primarily oleic acid), it also provides a substantial amount of SFAs (39.47%, palmitic acid and stearic acid). Lard is abundant in SFAs and MUFA, which may improve insulin sensitivity and help regulate blood glucose levels<sup>16</sup>. More importantly, from the perspectives of inflammation and lipid deposition, lard also has a relatively higher n-3/n-6 ratio (0.007) compared with camellia seed oil (0.004) and peanut oil (0.002). Since n-6 PUFA serve as the main precursors of proinflammatory lipid mediators (e.g., prostaglandins, leukotrienes) and excessive n-6 intake exacerbates tissue inflammation<sup>17</sup>, lard's favorable n-3/n-6 ratio suggests it provides fewer proinflammatory n-6 precursors under the same energy intake, potentially reducing inflammatory signal activation. This advantage is further supported by our prior findings: an appropriate mixture of lard and sunflower oil (high in n-6 PUFA) significantly reduced hepatic triglyceride accumulation, serum free fatty acid levels, and adipose tissue hypertrophy—exhibiting better anti-lipid deposition effects than sunflower oil alone<sup>18</sup>. This confirms that lard's fatty acid profile, when used in a certain proportion, inhibits excessive lipid accumulation and alleviates lipid overload-induced inflammation. In contrast, camellia seed oil supplementation led to reductions in both body weight and lean mass. Camellia seed oil contains a higher

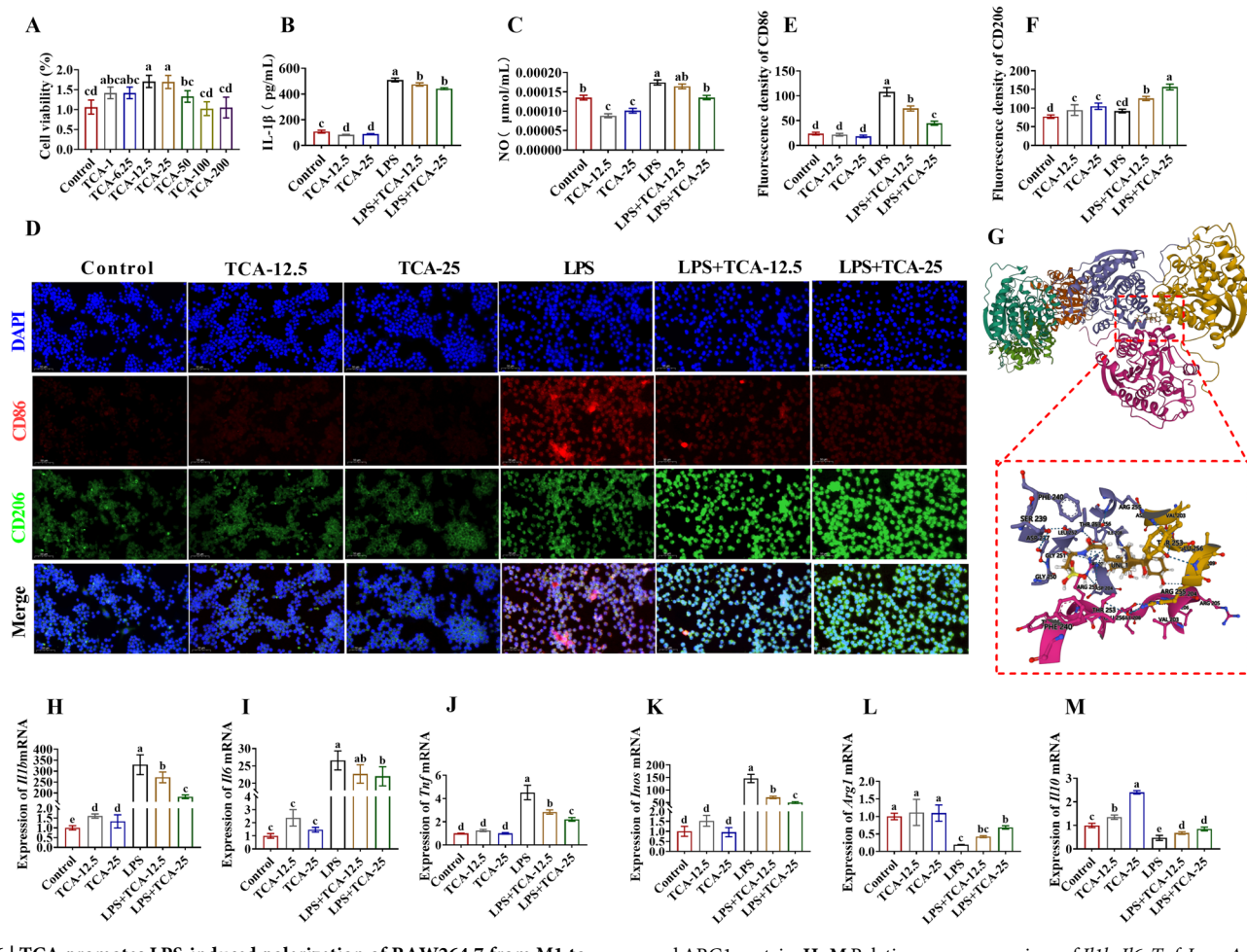


**Fig. 6 | TCA promotes LPS-induced polarization of RAW264.7 from M1 to M2 type. A CCK8 cell viability assay. B IL-1 $\beta$  content. C NO content. D Immunofluorescence double staining of CD86 and CD206 (200 $\times$ ). E, F Fluorescence intensity statistics of CD86 and CD206. G 3D interactions of TCA.**

and ARG1 protein. H–M Relative genes expressions of *Il1b*, *Il6*, *Tnf*, *Inos*, *Arg1*, *Il10*. Superscript letters (a, b, c, d and e) indicate significant differences between groups at  $P < 0.05$ .

MUFAs proportion of oleic acid (OA) (81.28%) and lower SFAs content (11.34%), which may alter energy partitioning and affect muscle metabolism, but the weight reduction may benefit from high OA levels<sup>19</sup>. Notably, however, camellia seed oil's n-6 PUFAs account for 99.6% of its total PUFAs, with extremely low n-3 PUFA content—resulting in an n-3/n-6 ratio lower than that of lard. This makes it likely to provide more proinflammatory precursors during long-term high intake, which may explain why camellia seed oil intake increased lipid deposition in mice compared with lard in our study. Peanut oil showed less pronounced changes in body weight and lean mass compared with the other two oils. It is worth noting that peanut oil supplementation resulted in an intermediate phenotype for some parameters. For instance, its effect on reducing lean mass was less dramatic than that of camellia seed oil, which might be partially related to its linoleic acid content (29.17%). In vivo studies have reported that supplementing the diet of colon-26 adenocarcinoma-bearing mice, a model for cancer cachexia, with conjugated linoleic acid helps maintain gastrocnemius muscle mass<sup>20</sup>. However, it is critical to distinguish that the high level of standard linoleic acid in peanut oil may not recapitulate the same effects, and our data do not support a protective effect of peanut oil on lean mass superior to lard. Although Yang et al.<sup>21</sup> reported that a high-fat diet containing 60% MUFAs maintained blood lipid levels and potentially inhibited lipid deposition in obese hamsters by enhancing lipolytic enzyme activity. Notably, in our study, compared with lard, the intake of Camellia seed oil increased the lipid deposition in mice. Different from the short-term feeding with a high-fat diet in most studies, this study employed long-term feeding with a

moderate-low fat diet, which may explain the observed phenotypic differences.

Obesity is characterized by excessive lipid accumulation in white adipose tissue (WAT), primarily caused by an energy intake and expenditure imbalance. Lipid synthesis in mammals is strictly regulated by the sterol regulatory element-binding proteins (SREBPs) family<sup>22</sup>. SREBP-1c primarily induces the expression of genes related to fatty acid synthesis in mammals<sup>23,24</sup>. This study found that *Srebp-1c* gene expression in the Camellia seed oil group was markedly increased. The upregulation of SREBP-1c expression can also significantly increase the expression of FASN and SCD1, further promoting lipid deposition<sup>25,26</sup>, which is consistent with the results of this study. Adipolysis breaks down TG stored in adipocytes, releasing fatty acids and glycerol. The mobilization of adipose tissue is mainly mediated by ATGL, HSL, and monoglyceride lipase (MGL)<sup>27</sup>. Fatty acid  $\beta$ -oxidation is the primary decomposition pathway in the body, with CPT1 serving as the rate-limiting enzyme for this process<sup>28</sup>. ACS enzymes activate fatty acids into acyl-CoA, facilitating mitochondrial oxidation<sup>29</sup>. Notably, lard intake significantly upregulates *Hsl*, *Atgl*, *Cat*, *Cpt1*, and *Acs* mRNA levels, thereby reducing lipid deposition.

Obesity induces systemic oxidative stress, causing the accumulation of ROS and an inflammatory response<sup>30,31</sup>. In this study, lard intake enhanced in vivo antioxidant capacity, reduced oxidative stress, and mitigated adipose inflammation. Emerging evidence highlights a close link between adipose inflammation and macrophages, particularly in obesity-related metabolic disorders<sup>32–34</sup>. Adipose tissue contains various immune cell populations,

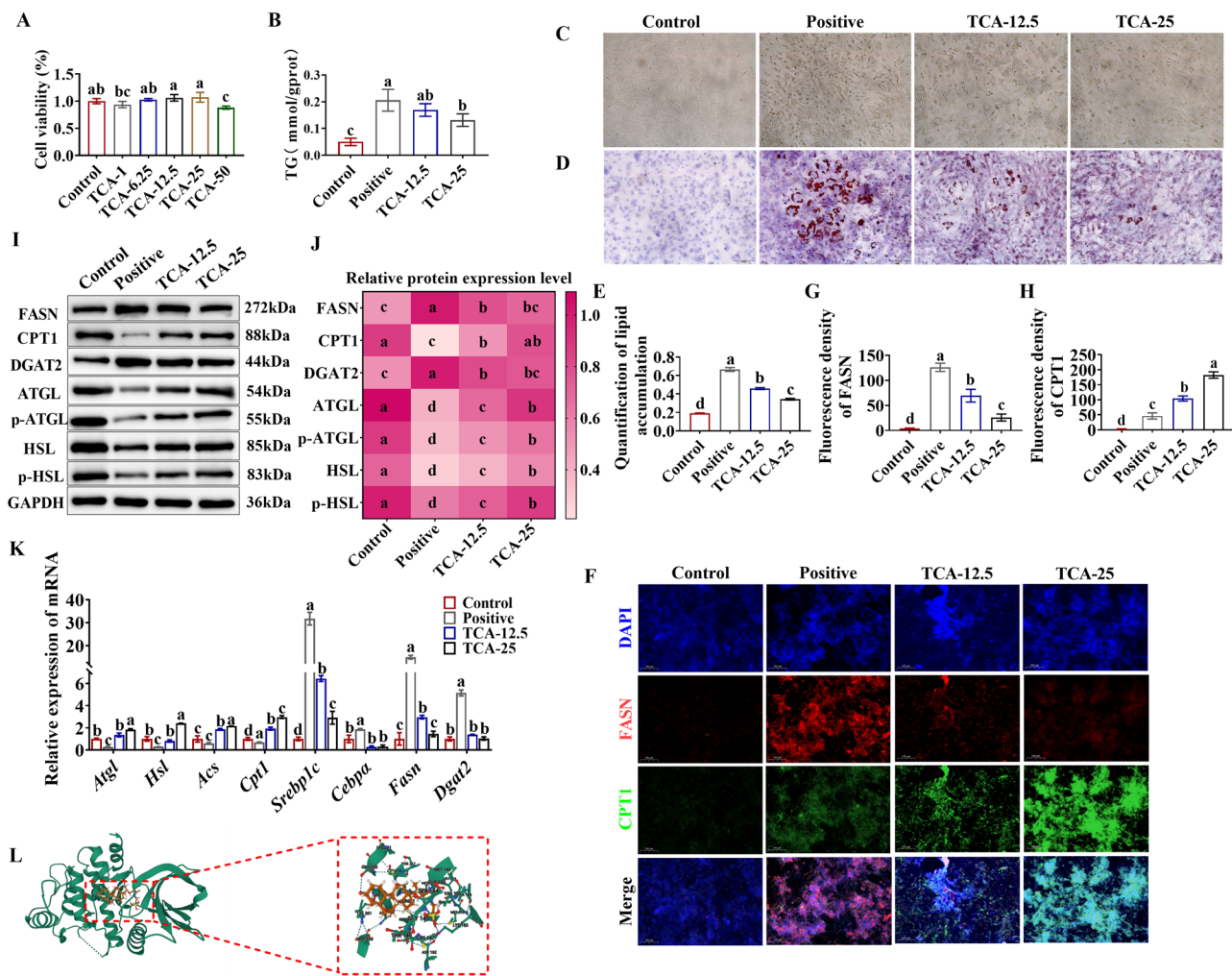


**Fig. 7 | TCA inhibits lipogenesis in 3T3-L1 cells. A** CCK8 cell viability assay. **B** TG content. **C** Cell morphology observation (100x). **D** Oil Red O Staining (100x). **E** Lipid accumulation was quantified by measuring the absorbance at 510 nm. **F** Immunofluorescence double staining of FASN and CPT1 (100x). **G, H** Fluorescence intensity statistics of FASN and CPT1. **I, J** Relative protein

expressions of FASN, CPT1, DGAT2, ATGL, P-ATGL, HSL, P-HSL. **K** Relative gene expressions of *Atgl*, *Hsl*, *Acs*, *Cpt1*, *Srebp1c*, *Cebpa*, *Fasn*, *Dgat2*. **L** 3D interactions of TCA and CPT1 protein. Superscript letters (a, b, c and d) indicate significant differences between groups at  $P < 0.05$ .

among which macrophages are the most predominant and are specifically termed adipose tissue macrophages (ATMs). Under normal conditions, macrophages make up 5% to 10% of adipose tissue, and this proportion can increase to 50% or more in extremely obese humans and mice<sup>35,36</sup>. Within adipose tissue, activated macrophages are classified into two phenotypes: M1 macrophages and M2 macrophages. In the adipose tissue of lean mice, M2 macrophages predominate, producing anti-inflammatory cytokines such as IL-10 and transforming growth factor- $\beta$  (TGF- $\beta$ ), contributing to the resolution of inflammation. However, in obese mice, adipose tissue recruits a large number of M1 macrophages, which secrete pro-inflammatory factors, leading to inflammation and metabolic dysfunction in adipose tissue<sup>37-39</sup>. Our study showed that Camellia seed oil and peanut oil promoted ATM polarization toward the M1 phenotype, upregulating *Inos*, *Il6*, *Il1b*, and *Tnf*. Conversely, lard promoted M2 polarization, increasing *Il10*, *Arg1*, *Mrc1*, and *Mrc2*. Consequently, Camellia seed oil-fed mice exhibited higher CD86 expression and a lower CD206/CD11c ratio than lard- and peanut oil-fed groups. However, from the overall results, peanut oil presented a mixed profile. While it did not induce the severe lean mass loss seen with camellia seed oil, it consistently underperformed compared with lard in key aspects of adipose tissue homeostasis. As it possesses the highest n-6 PUFA content (29.23%) among the three oils, its pro-inflammatory potential was evident. This was corroborated by our adipose

tissue inflammation results, which showed its anti-inflammatory effect was inferior to that of the lard group, with elevated ROS production, increased the expression level of *Il6* and a reduced presence of M2 macrophages (e.g., lower CD206). Furthermore, histological analysis revealed increased adipocyte size in peanut oil-fed mice compared with the lard group, indicating exacerbated adipose tissue hypertrophy. These findings indicate that lard mitigates adipose inflammation by promoting M2 polarization, whereas chronic Camellia seed oil intake enhances lipid deposition, inducing subsequent adipose inflammation. In contrast, while peanut oil's effects differed from those of camellia seed oil in some aspects (e.g., lean mass), its overall metabolic profile was less favorable than lard's and did not exhibit the same compelling, multi-faceted advantage that warranted an in-depth mechanistic exploration. We aimed to prioritize the investigation of the fat source that most effectively maintained adipose tissue homeostasis, which was lard. The newly identified mechanism involving TCA provides a novel explanation for lard's superior effects.

TCA is a conjugated form of **cholic acid** with taurine, and it is also a dominant conjugate form of bile acids in humans<sup>40</sup>. TCA is significant as an antidiabetic medication in T1D management. The incorporation of TCA into G-microcapsules exerted positive effects on cell viability and glycemic control in Type-1 diabetic animals<sup>41</sup>. Under hyperglycemia, TCA also assisted Probucol, a lipophilic drug in an animal model of T2D, to enhance

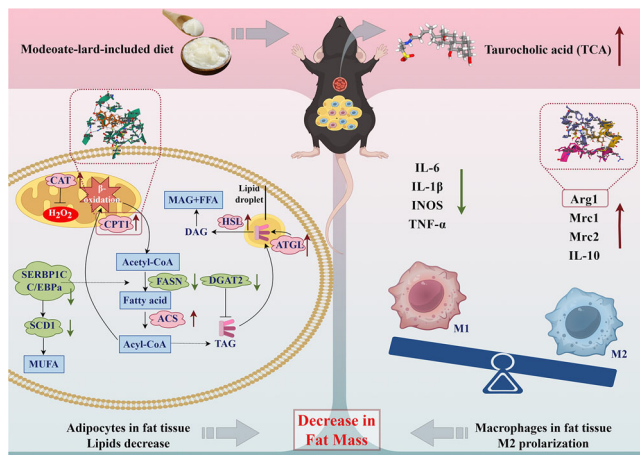


**Fig. 8 | Mechanism by which a moderate lard-included diet reduces fat deposition and inflammation in the adipose tissue.** The upward arrow indicates positive correlation, while the downward arrow indicates negative correlation (By Figdraw).

stability, improve  $\beta$ -cell survival, reduced the pro-inflammatory cytokine TNF- $\alpha$ , and desirable targeted release properties of probucol<sup>42</sup>. Another study found that TCA supplementation in the paraventricular nucleus of spontaneously hypertensive rats can mitigate inflammation and oxidative stress, inhibits neuron activation, and reduce hypertension<sup>43</sup>. In our results, TCA is the key differential metabolite in lard group. We used LPS to induce inflammation in RAW 264.7 macrophages, pretreatment with TCA significantly reduced the expression of M1 macrophage markers, while significantly increased the expression of M2 macrophages marker in the supernatant of LPS-induced RAW264.7 cells. Bile acids have been shown to enhance energy expenditure, boost insulin sensitivity, and reduce fasting lipemia<sup>44</sup>. Long-term taurine feeding reduces plasma cholesterol and bile acid levels and effectively prevents hypercholesterolemia<sup>45</sup>. We speculate that TCA can reduce lipid deposition. Our study observed an increase in lipid droplet numbers, mRNA expression levels of *Srebp-1c*, *Fasn*, *Scd1*, *Dgat2*, and *Cebpa*, along with TG content in untreated cells during differentiation. TCA treatment led to a reduction in these parameters, alongside significantly elevated mRNA expression of *Atgl*, *Hsl*, *Cpt1*, and *Acs*. The findings indicate that TCA potentially suppresses adipogenesis by modulating the expression of transcription factors related to adipocyte differentiation and lipid deposition.

In addition to the tissue-specific alterations observed, it is essential to consider how adipocyte-derived metabolites influence whole-body homeostasis. The surge in lipolysis induced by the dietary oils leads to elevated circulating free-fatty acids (FFAs), which are readily taken up by the liver and skeletal muscle, where they can be re-esterified into triglycerides, contributing to hepatic steatosis and intramyocellular lipid accumulation—key drivers of insulin resistance<sup>46,47</sup>. Moreover, excess FFAs act as ligands for Toll-like-receptor 4 and other pattern-recognition receptors, promoting a shift toward pro-inflammatory M1 macrophage polarization and the release of cytokines such as TNF- $\alpha$  and IL-6. These inflammatory signals further impair insulin signaling pathways, creating a vicious cycle of metabolic dysfunction<sup>48,49</sup>. Our data show that lard uniquely raises serum TCA, a molecule reported to dampen M1 activation and enhance M2 polarization, thereby partially offsetting the deleterious systemic impact of heightened FFAs. Conversely, camellia seed oil and peanut oil, with their low n-3/n-6 ratios and predominance of n-6 polyunsaturated fatty acids, generate an FFA profile that favors M1 polarization and oxidative stress, suggesting that their adipose-tissue benefits may be outweighed by adverse systemic effects. This underscores the necessity of evaluating dietary interventions not only for local adipose outcomes but also for their broader metabolic repercussions. We will investigate the effects of lard intake on lipid accumulation in liver and skeletal muscle, systemic insulin sensitivity and serum lipid

spectrum, which will help to clarify whether the benefits of adipose tissue translate into systemic metabolic health.

In the dietary pattern where dietary fat constitutes 25% of energy intake, lard consumption, as opposed to camellia seed oil and peanut oil, significantly elevates plasma TCA levels. This elevation subsequently enhances the expression of genes related to lipolysis and promotes the polarization of M2 macrophages within adipose tissue, thereby markedly reducing inflammatory markers and lipid accumulation. While peanut oil exhibits a certain advantage in maintaining muscle mass, the proinflammatory effects caused by its high n-6 PUFA ratio limit its overall metabolic benefits. These findings challenge the conventional view of animal fats and demonstrate that consuming lard at the recommended level (with dietary fat providing 25% of energy) can confer metabolic benefits by regulating adipose tissue homeostasis (Fig. 8). This study provides evidence-based insights into the selection and consumption levels of dietary oils.

## Methods

### Chemicals and reagents

Table S1 contains a list of the main reagents and antibodies used.

### Animals, diets, and experimental procedure

The 7w male C57BL/6 mice (purchased from Hunan SJA Laboratory Animal Co., Ltd, Hunan, China) (SCXK (Xiang) 2019-0004) were maintained in a specific pathogen-free animal facility. All mice were kept under aseptic conditions with free access to food and water. After a week of adaptive feeding, the mice were randomly divided into three experimental groups ( $n = 9$  each). Lard, Camellia seed oil, and peanut oil were used as experimental oils, and the mice were fed with a whole food diet containing 25% fat energy, respectively, for 24 weeks. The mice were sacrificed after fasting for 6 hours. All animal experiments followed the Animal Welfare and Use Guidelines of China and were approved by the Animal Welfare Committee of Hunan Agricultural University (Approval Number: 43322108). Whole food diets were produced by Trophic Animal Feed High-Tech Co., Ltd. (Nantong, China). Refer to Table S2 for the diet formulas.

### Sample collection

Mice were weighed before dissection. Before sacrifice via cervical dislocation, the mice were anesthetized intraperitoneally with a 1.25% sodium tribromoethanol solution (MeilunBio, Dalian, China) at a dose of 0.2 mL/10 g body weight. Subsequently, orbital blood samples, white adipose tissues (including epididymal fat, perirenal fat, and subcutaneous fat), and brown adipose tissue were harvested. The tissues were preserved at -80°C for subsequent analysis.

### Fatty acid composition detection

Oil samples (100 mg) were hydrolyzed with HCl/ethanol (80°C, 45 min), and then transesterified with KOH/methanol. Fatty acid methyl esters (FAMEs) were extracted with hexane and analyzed by GC-MS (Agilent 8860/5977B; HP-88 column; 140–240°C gradient). Peaks were identified using FAME standards and quantified via external calibration. Method validation showed good reproducibility (RSD < 5%) and sensitivity (LOD 0.01–0.05 µg/mL).

### Histology staining for adipose tissue

Fixed subcutaneous fat samples were dehydrated, paraffin-embedded, and sectioned (3–5 µm thickness). Sections were stained with hematoxylin and eosin (H&E) following standard protocols. Histomorphometric analysis was performed using light microscopy and quantified with ImageJ software<sup>10</sup>.

### Biochemical assays for oxidative stress markers

Adipose tissue samples stored at -80°C were thawed, and Reactive Oxygen Species (ROS) levels were measured using a commercial ELISA kit. Additionally, Malondialdehyde (MDA), Superoxide Dismutase (SOD) and

Reduced glutathione (GSH) activities were determined following the manufacturer's instructions<sup>50</sup>.

### Metabolomics analysis

Serum metabolites were extracted with 400  $\mu$ L methanol: acetonitrile (1:1, v/v) and analyzed by UHPLC-Q Exactive mass spectrometry (Thermo Fisher Scientific). Metabolites were identified by matching MS/MS spectra against HMDB, METLIN, and Majorbio's internal database. Data were processed on the Majorbio Cloud Platform<sup>51</sup>.

### Cell culture and differentiation

3T3-L1 pre-adipocytes were sourced from the Second Xiangya Hospital of Central South University (Changsha, China) and cultured in DMEM containing 10% FBS and 1% antibiotics. To promote adipocyte differentiation, 3T3-L1 cells at full confluence (day 0) treated with MDI induction medium (containing 0.5 mM isobutylmethylxanthine (IBMX) 1  $\mu$ M dexamethasone, and 10  $\mu$ g/mL insulin) for 48 hours, then maintained in DMEM-High Glucose medium with 10  $\mu$ g/mL insulin for an additional 48 hours. The cells were cultured in standard growth medium, with the medium containing 10  $\mu$ g/mL insulin replaced every two days, until they fully differentiated into mature adipocytes by day 8. The experiment was divided into the following groups: control, positive, TCA-12.5  $\mu$ M, and TCA-25  $\mu$ M. For the TCA intervention study, cells were treated with various concentrations of TCA (12.5 and 25  $\mu$ M) simultaneously with adipogenic induction at the beginning of differentiation. The positive control group received an equal volume of complete medium without TCA, while undergoing adipogenic induction simultaneously, and thus served as the positive control for adipocyte differentiation. In contrast, the control group was given an equal volume of complete medium without TCA, with no adipogenic induction applied.

RAW 264.7 cells were sourced from the Institute of Subtropical Agriculture, Chinese Academy of Sciences National (Changsha, China) and cultured in 1640 containing 10% FBS and 1% antibiotics. Experiments commenced when RAW 264.7 cells, seeded in 6-well plates, achieved 70-80% confluence. TCA at concentrations of 12.5 and 25  $\mu$ M was pre-activated for 2 hours before adding 1  $\mu$ g/mL of LPS solution to each well for a 24-hour co-stimulation to induce the M1 phenotype. The experiment was divided into the following groups: control, TCA-12.5  $\mu$ M, TCA-25  $\mu$ M, LPS + TCA-12.5  $\mu$ M, and LPS + TCA-25  $\mu$ M, with a total treatment of 24 h.

### Cell viability

Cell viability at each TCA density (0, 1, 6.25, 12.5, 25, 50  $\mu$ M) was evaluated using a cell counting kit. After seeding the cells on a 96-well culture plate for 24 h, the cells were washed with PBS. Add fresh medium containing 0.1 mL/ml CCK-8, incubation for 1 h, the intensity was measured at a wavelength of 450 nm.

### Oil red O staining

On day 8 after differentiation induction, 3T3-L1 cells underwent PBS washing, 20-minute fixation with 10% formalin, followed by a wash with 60% isopropyl alcohol. Oil red O staining followed the manufacturer's guidelines. Photomicrographs were obtained using an inverted microscope (Nikon, Tokyo, Japan). Subsequently, 300  $\mu$ L of pure isopropyl alcohol was added to each well for lipid extraction, followed by a 20-fold dilution, and the absorbance was measured at 510 nm using a microplate reader.

### Measurement of intracellular triglyceride levels

On day 8, after differentiation induction, cells were disrupted using lysis buffer. The intracellular triglyceride (TG) content was measured using a TG determination kit in accordance with the manufacturer's instructions. The absorbance was measured at 500 nm using a microplate reader.

### Generation of nitric oxide and IL-1 $\beta$ level assays

According to the NO detection kit and the enzyme-linked immunosorbent assay (ELISA) kits of mouse IL-1 $\beta$ , RAW264.7 cells were cultured overnight in 96-well plates, and then exposed to different concentrations of TCA and LPS (1  $\mu$ g/mL) individually or in combination for 24 h. The absorbance of each group was measured at 550 nm for NO detection. The plates were read at 450 nm for IL-1 $\beta$  detection.

### Immunofluorescence staining for adipose tissue, 3T3-L1 cell and RAW 264.7 cell

Cells were fixed with 4% paraformaldehyde for 15 minutes at room temperature and washed with PBS 3 times. Following dewaxing to water for paraffin-embedded sections of adipose tissue, antigen retrieval was performed in citrate antigen retrieval buffer. After blocking both the adipose tissue and cells, the primary antibody was applied, followed by the secondary antibody. After incubation, DAPI staining solution was added to counterstain the nuclei for 10 minutes and visualized using fluorescent microscopy (Olympus, Tokyo, Japan). Fluorescence images were captured using Image-J software, with five different fields per sample analyzed for quantification

### qPCR

Total RNA was extracted from subcutaneous adipose tissue, 3T3-L1 and RAW 264.7 cells by TRIzol, and RNA was reverse transcribed into cDNA using a PrimeScript RT reagent kit with gDNA Eraser. Genes were selected (Table S3) for qPCR analyses: *Actb*, *Fasn*, *Dgat2*, *Cebpa*, *Scd1*, *Srebp1c*, *Hsl*, *Cat*, *Atgl*, *Acc*, *Cpt1*, *Ucp1*, *Fndc5*, *Prdm16*, *Ppargc1a*, *Ampk*, *Inos*, *Il6*, *Tnf*, *Il1b*, *Il10*, *Arg1*, *Mrc1*, *Mrc2*. The details of total RNA extraction, cDNA preparation and qPCR assays are described in the previous study<sup>4</sup>.

### Western blotting

Western blotting was performed as described previously<sup>52</sup>. Finally, detection was visualized by using the ECL chemical luminescent detection kit, and the bands were further analyzed using Image-J software. Antibodies are shown in Table S1.

### Molecular docking

To analyze the binding affinities and modes of interaction between the drug candidate and their targets, AutodockVina 1.2.2, a silico protein-ligand docking software, was employed. The molecular structures of TCA were retrieved from PubChem Compound (<https://pubchem.ncbi.nlm.nih.gov>). The 3D coordinates of CPT1 (PDB ID, 6YG3; resolution, 2.05  $\text{\AA}$ ) and ARG1 (PDB ID, 8E5M; resolution, 1.84  $\text{\AA}$ ) were downloaded from the PDB (<http://www.rcsb.org/pdb/home/home.do>). For docking analysis, all protein and molecular files were converted into PDBQT format with all water molecules excluded and polar hydrogen atoms were added. The grid box was centered to cover the domain of each protein and to accommodate free molecular movement. Molecular docking studies were performed by Autodock Vina 1.2.2 (<http://autodock.scripps.edu>).

### Statistical analyses

All quantitative data are presented as means  $\pm$  standard deviation (SD) from three independent replicates. Data were tested for normality using the Shapiro-Wilk test. Normally distributed data were analyzed using one-way analysis of variance (ANOVA). Non-normally distributed data were analyzed using the Kruskal-Wallis rank-sum test. Differences between two groups were analyzed using Student's t test. GraphPad Prism (version 9; GraphPad Software, CA, USA) was used for data analysis.  $P < 0.05$  was considered to be significant.

### Data availability

The authors declare that the data supporting the findings of this study are available within the article.

Received: 14 June 2025; Accepted: 28 November 2025;

Published online: 12 December 2025

## References

- Piché, M. E., Tchernof, A. & Després, J. P. Obesity phenotypes, diabetes, and cardiovascular diseases. *Circ. Res.* **126**, 1477–1500 (2020).
- Welsh, A., Hammad, M., Piña, I. L. & Kulinski, J. Obesity and cardiovascular health. *Eur. J. Prevent. Cardiol.* **31**, 1026–1035 (2024).
- Zhang, L. et al. High-carbohydrate diet consumption poses a more severe liver cholesterol deposition than a high-fat and high-calorie diet in mice. *Int. J. Molecular Sci.* **24** <https://doi.org/10.3390/ijms241914700> (2023).
- Zhang, L. et al. Purified diet versus whole food diet and the inconsistent results in studies using animal models. *Food Funct.* **13**, 4286–4301 (2022).
- Yan, S. et al. Critique of the Chinese dietary guidelines on the consumption of cooking oils. *Food Sci. Nutr.* **9**, 583–585 (2021).
- Wang, J. et al. Anti-obesity effect of a traditional Chinese dietary habit-blending lard with vegetable oil while cooking. *Sci. Rep.* **7**, 14689 (2017).
- Guo, F. et al. It is time to reevaluate the lard in glucose homeostasis and diabetes pathogenesis. *NPJ Sci. Food* **8**, 109 (2024).
- Le Thuc, O. & García-Cáceres, C. Obesity-induced inflammation: connecting the periphery to the brain. *Nat. Metab.* **6**, 1237–1252 (2024).
- Xu, S., Lu, F., Gao, J. & Yuan, Y. Inflammation-mediated metabolic regulation in adipose tissue. *Obes. Rev. Off. J. Int. Assoc. Study Obes.* **25**, e13724 (2024).
- Wu, A. et al. Tannic acid mitigates *Salmonella*-induced lung injury via gut-lung axis in broilers. *Poult. Sci.* **104**, 104973 (2025).
- Liu, X. et al. Soybean oil induces neuroinflammatory response through brain-gut axis under high-fat diet. *J. Tradit. Complement. Med.* **14**, 522–533 (2024).
- Yan, S. et al. A lard and soybean oil mixture alleviates low-fat-high-carbohydrate diet-induced nonalcoholic fatty liver disease in mice. *Nutrients* **14** <https://doi.org/10.3390/nu14030560> (2022).
- Roh, H. T., Cho, S. Y. & So, W. Y. Obesity promotes oxidative stress and exacerbates blood-brain barrier disruption after high-intensity exercise. *J. Sport Health Sci.* **6**, 225–230 (2017).
- Xu, J. et al. Protective effects of taurocholic acid on excessive hepatic lipid accumulation via regulation of bile acid metabolism in grouper. *Food Funct.* **13**, 3050–3062 (2022).
- Coelho, O. G. L., Cândido, F. G. & Alfenas, R. C. G. Dietary fat and gut microbiota: mechanisms involved in obesity control. *Crit. Rev. Food Sci. Nutr.* **59**, 3045–3053 (2019).
- Ussar, S. & Tschoep, M. H. [Br]eaKing FAt. *Cell* **159**, 238–240 (2014).
- Saini, R. K. & Keum, Y. S. Omega-3 and omega-6 polyunsaturated fatty acids: Dietary sources, metabolism, and significance - A review. *Life Sci.* **203**, 255–267 (2018).
- Yan, S., Li, X., Zhang, L., Zeng, Y. & Wang, J. Moderate quantity of lard mixed with sunflower oil attenuate lipid accumulation in mice. *Oil Crop Sci.* **5**, 8 (2020).
- Tutunchi, H., Ostadrabimi, A. & Saghafi-Asl, M. The effects of diets enriched in monounsaturated oleic acid on the management and prevention of obesity: a systematic review of human intervention studies. *Adv. Nutr.* **11**, 864–877 (2020).
- Graves, E., Hitt, A., Pariza, M. W., Cook, M. E. & McCarthy, D. O. Conjugated linoleic acid preserves gastrocnemius muscle mass in mice bearing the colon-26 adenocarcinoma. *Res. Nurs. Health* **28**, 48–55 (2005).
- Yang, S. C., Lin, S. H., Chang, J. S. & Chien, Y. W. High fat diet with a high monounsaturated fatty acid and polyunsaturated/saturated fatty acid ratio suppresses body fat accumulation and weight gain in obese hamsters. *Nutrients* **9** <https://doi.org/10.3390/nu9101148> (2017).
- Shen, S. et al. SIRT1/SREBPs-mediated regulation of lipid metabolism. *Pharmacol. Res.* **199**, 107037 (2024).
- Gosis, B. S. et al. Inhibition of nonalcoholic fatty liver disease in mice by selective inhibition of mTORC1. *Science* **376**, eabf8271 (2022).
- Nguyen, T. T. P. et al. SREBP-1c impairs ULK1 sulfhydratation-mediated autophagic flux to promote hepatic steatosis in high-fat-diet-fed mice. *Mol. cell* **81**, 3820–3832.e3827 (2021).
- Zheng, Z. G. et al. Discovery of a potent SCAP degrader that ameliorates HFD-induced obesity, hyperlipidemia and insulin resistance via an autophagy-independent lysosomal pathway. *Autophagy* **17**, 1592–1613 (2021).
- Li, Q. et al. circPRKAA1 activates a Ku80/Ku70/SREBP-1 axis driving de novo fatty acid synthesis in cancer cells. *Cell Rep.* **41**, 111707 (2022).
- Haemmerle, G. et al. Defective lipolysis and altered energy metabolism in mice lacking adipose triglyceride lipase. *Science* **312**, 734–737 (2006).
- Ngo, J. et al. Mitochondrial morphology controls fatty acid utilization by changing CPT1 sensitivity to malonyl-CoA. *EMBO J.* **42**, e111901 (2023).
- Chen, J. et al. ACSL4 reprograms fatty acid metabolism in hepatocellular carcinoma via c-Myc/SREBP1 pathway. *Cancer Lett.* **502**, 154–165 (2021).
- de Mello, A. H., Costa, A. B., Engel, J. D. G. & Rezin, G. T. Mitochondrial dysfunction in obesity. *Life Sci.* **192**, 26–32 (2018).
- Masenga, S. K., Kabwe, L. S., Chakulya, M. & Kirabo, A. Mechanisms of oxidative stress in metabolic syndrome. *Int. J. Molecular Sci.* **24** <https://doi.org/10.3390/ijms24097898> (2023).
- Kern, P. A., Ranganathan, S., Li, C., Wood, L. & Ranganathan, G. Adipose tissue tumor necrosis factor and interleukin-6 expression in human obesity and insulin resistance. *Am. J. Physiol. Endocrinol. Metab.* **280**, E745–E751 (2001).
- Ou, M. Y., Zhang, H., Tan, P. C., Zhou, S. B. & Li, Q. F. Adipose tissue aging: mechanisms and therapeutic implications. *Cell Death Dis.* **13**, 300 (2022).
- Kawai, T., Autieri, M. V. & Scalia, R. Adipose tissue inflammation and metabolic dysfunction in obesity. *Am. J. Physiol. Cell Physiol.* **320**, C375–C391 (2021).
- Yao, J., Wu, D. & Qiu, Y. Adipose tissue macrophage in obesity-associated metabolic diseases. *Front. Immunol.* **13**, 977485 (2022).
- Liang, W. et al. The roles of adipose tissue macrophages in human disease. *Front. Immunol.* **13**, 908749 (2022).
- Wang, Y., Smith, W., Hao, D., He, B. & Kong, L. M1 and M2 macrophage polarization and potentially therapeutic naturally occurring compounds. *Int. Immunopharmacol.* **70**, 459–466 (2019).
- Vogel, A., Brunner, J. S., Hajto, A., Sharif, O. & Schabbauer, G. Lipid scavenging macrophages and inflammation. *Biochim. Biophys. Acta Mol. Cell Biol. Lipids* **1867**, 159066 (2022).
- Watanabe, S., Alexander, M., Misharin, A. V. & Budinger, G. R. S. The role of macrophages in the resolution of inflammation. *J. Clin. Investig.* **129**, 2619–2628 (2019).
- Sarkar, P., Basak, P., Ghosh, S., Kundu, M. & Sil, P. C. Prophylactic role of taurine and its derivatives against diabetes mellitus and its related complications. *Food Chem. Toxicol. Int. J. Published Br. Ind. Biol. Res. Assoc.* **110**, 109–121 (2017).
- Mathavan, S., Chen-Tan, N., Arfuso, F. & Al-Salami, H. A comprehensive study of novel microcapsules incorporating gliclazide and a permeation enhancing bile acid: hypoglycemic effect in an animal model of Type-1 diabetes. *Drug Deliv.* **23**, 2869–2880 (2016).
- Mooranian, A., Negulj, R., Arfuso, F. & Al-Salami, H. The effect of a tertiary bile acid, taurocholic acid, on the morphology and physical characteristics of microencapsulated probucol: potential applications in diabetes: a characterization study. *Drug Deliv. Transl. Res.* **5**, 511–522 (2015).
- Li, Y. et al. Taurocholic acid ameliorates hypertension through the activation of TGR5 in the hypothalamic paraventricular nucleus. *Food Funct.* **15**, 5088–5102 (2024).

44. Farr, S. et al. Bile acid treatment and FXR agonism lower postprandial lipemia in mice. *Am. J. Physiol. Gastrointest. Liver Physiol.* **318**, G682–g693 (2020).

45. Tagawa, R. et al. Long-term dietary taurine lowers plasma levels of cholesterol and bile acids. *Int. J. Molecular Sci.* **23** <https://doi.org/10.3390/ijms23031793> (2022).

46. Bays, H. E. et al. Obesity, dyslipidemia, and cardiovascular disease: a joint expert review from the obesity medicine association and the national lipid association 2024. *Obes. pillars* **10**, 100108 (2024).

47. Lopez-Yus, M., Hörndl, C., Borlan, S., Bernal-Monterde, V. & Arbones-Mainar, J. M. Unraveling adipose tissue dysfunction: molecular mechanisms, novel biomarkers, and therapeutic targets for liver fat deposition. *Cells* **13** <https://doi.org/10.3390/cells13050380> (2024).

48. Engin, A. B. Message transmission between adipocyte and macrophage in obesity. *Adv. Exp. Med. Biol.* **1460**, 273–295 (2024).

49. Engin, A. Reappraisal of adipose tissue inflammation in obesity. *Adv. Exp. Med. Biol.* **1460**, 297–327 (2024).

50. Wang, J. et al. Tannic acid ameliorates systemic glucose and lipid metabolic impairment induced by low-dose T-2 toxin exposure. *J. Agric. Food Chem.* **71**, 12574–12586 (2023).

51. Zhou, Y. et al. Metabolomic and transcriptomic analysis of effects of three MUFA-rich oils on hepatic glucose and lipid metabolism in mice. *Mol. Nutr. Food Res.* **67**, e2300398 (2023).

52. Xu, Q. et al. An *Ilex latifolia*-containing compound tea regulates glucose-lipid metabolism and modulates gut microbiota in high-fat diet-fed mice. *Food Front.* **5**, 802–819 (2024).

## Acknowledgements

We would like to thank the National Natural Science Foundation of China (Grant No.32373079), and the Horizontal Scientific Research Projects (No. 2019xny-js044) for financial support. We would also like to thank Hunan Wonderwave Biotechnology Co., Ltd. for their histopathological techniques support.

## Author contributions

X.Y.L.: Writing—original draft, Methodology, Formal analysis, Data curation. S.L.: Software, Investigation, Formal analysis, Data curation. J.W.W.: Validation, Data curation. L.X.: Writing—review & editing. Z.Q.H.: Data

curation. Y.L.D.: Data curation. R.Z.: Software. Q.R.X.: Methodology. S.S.Y.: Investigation. X.W.L.: Investigation, Data curation. L.X.W.: Supervision, Funding acquisition. J.W.: Investigation, Formal analysis, Conceptualization.

## Competing interests

The authors declare no competing interests.

## Additional information

**Supplementary information** The online version contains supplementary material available at <https://doi.org/10.1038/s41538-025-00657-8>.

**Correspondence** and requests for materials should be addressed to Lixin Wen or Ji Wang.

**Reprints and permissions information** is available at <http://www.nature.com/reprints>

**Publisher's note** Springer Nature remains neutral with regard to jurisdictional claims in published maps and institutional affiliations.

**Open Access** This article is licensed under a Creative Commons Attribution-NonCommercial-NoDerivatives 4.0 International License, which permits any non-commercial use, sharing, distribution and reproduction in any medium or format, as long as you give appropriate credit to the original author(s) and the source, provide a link to the Creative Commons licence, and indicate if you modified the licensed material. You do not have permission under this licence to share adapted material derived from this article or parts of it. The images or other third party material in this article are included in the article's Creative Commons licence, unless indicated otherwise in a credit line to the material. If material is not included in the article's Creative Commons licence and your intended use is not permitted by statutory regulation or exceeds the permitted use, you will need to obtain permission directly from the copyright holder. To view a copy of this licence, visit <http://creativecommons.org/licenses/by-nc-nd/4.0/>.

© The Author(s) 2025